Cell Reports

Condensin Relocalization from Centromeres to Chromosome Arms Promotes Top2 Recruitment during Anaphase

Graphical Abstract

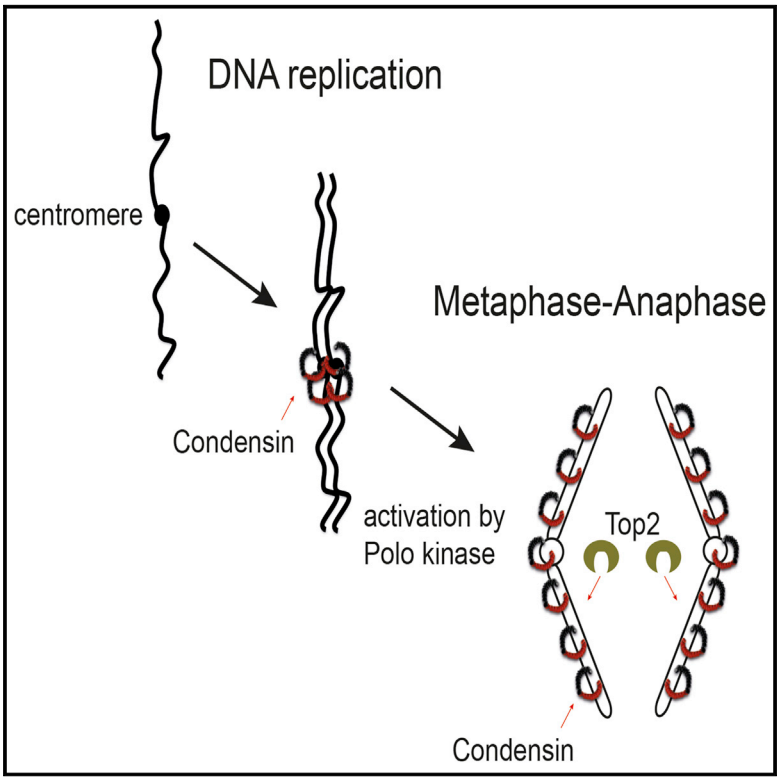

Authors

Joanne Leonard, Nicholas Sen, Raul Torres, Takashi Sutani, Adam Jarmuz, Katsuhiko Shirahige, Luis Aragón

Correspondence

luis.aragon@csc.mrc.ac.uk

In Brief

Chromosome condensation requires condensin and topoisomerase 2 (Top2) and is necessary for segregation. Leonard et al. show that condensin localizes to yeast centromeres following DNA replication and spreads to chromosome arms during anaphase when Top2 is also recruited. Condensin and Top2 activities are coordinated to shape mitotic chromosomes.

Highlights

- Condensin recruitment to centromeric regions requires DNA replication
- Centromeric condensin spreads to chromosome arms during anaphase
- Condensin promotes recruitment of Top2 during anaphase
- Condensin localization requires Polo kinase and correlates with DNA overwinding

Leonard et al., 2015, Cell Reports *13*, 2336–2344
December 22, 2015
http://dx.doi.org/10.1016/j.celrep.2015.11.041

CellPress

OPEN ACCESS
CellPress

Cell Reports
Report

Condensin Relocalization from Centromeres to Chromosome Arms Promotes Top2 Recruitment during Anaphase

Joanne Leonard,[1] Nicholas Sen,[1] Raul Torres,[1] Takashi Sutani,[2] Adam Jarmuz,[1] Katsuhiko Shirahige,[2] and Luis Aragón[1,*]
[1]Cell Cycle Group, Medical Research Council (MRC), Clinical Sciences Centre, Imperial College London, Hammersmith Hospital, Du Cane Road, London W12 0NN, UK
[2]Research Center for Epigenetic Disease, Institute of Molecular and Cellular Biosciences, The University of Tokyo, Tokyo 113-0032, Japan
*Correspondence: luis.aragon@csc.mrc.ac.uk
http://dx.doi.org/10.1016/j.celrep.2015.11.041

SUMMARY

Condensin is a conserved chromosomal complex necessary to promote mitotic chromosome condensation and sister chromatid resolution during anaphase. Here, we report that yeast condensin binds to replicated centromere regions. We show that centromeric condensin relocalizes to chromosome arms as cells undergo anaphase segregation. We find that condensin relocalization is initiated immediately after the bipolar attachment of sister kinetochores to spindles and requires Polo kinase activity. Moreover, condensin localization during anaphase involves a higher binding rate on DNA and temporally overlaps with condensin's DNA overwinding activity. Finally, we demonstrate that topoisomerase 2 (Top2) is also recruited to chromosome arms during anaphase in a condensin-dependent manner. Our results uncover a functional relation between condensin and Top2 during anaphase to mediate chromosome segregation.

INTRODUCTION

Mitotic chromosome condensation involves a dramatic reorganization of chromatin strands into compact chromosomes. Chromosome condensation is mediated by the condensin complex (Hirano, 2005) and is necessary to prevent sister chromatids from being entangled during segregation. In budding yeast, condensin is a five-subunit complex containing a pair of SMC ATPases (Smc2 and Smc4) and several non-SMC proteins (Brn1, Ycg1, and Ycs4) (Freeman et al., 2000). In addition to condensin (condensin I), most eukaryotic species contain a second condensin complex, condensin II, with different non-SMC protein subunits (Ono et al., 2003). Importantly, in higher eukaryotes both condensin complexes collaborate to shape mitotic chromosomes (Shintomi and Hirano, 2011).

One of the functions attributed to chromosome condensation is the removal of entanglements between replicated chromatids (Koshland and Strunnikov, 1996) that arise as a consequence of DNA replication (Sundin and Varshavsky, 1980). These entanglements or sister chromatid intertwines (SCI) can only be resolved by type IIA topoisomerases (such as Top2 in yeast) because of their ability to transiently break DNA strands and pass double helices through the break before religation (Wang, 2002). Therefore chromosome condensation, and condensin itself, has been thought to facilitate the role of Top2 in removing SCIs (Nasmyth, 2001).

However, the functional relation between Top2 and condensin is not fully understood. The consequences of Top2 and condensin ablation impairing yeast chromosome organization and segregation carry significant resemblance (Freeman et al., 2000; Holm et al., 1985; Saka et al., 1994; Uemura et al., 1987) thus suggesting functional cooperation between these two factors. Inactivation of condensin has been shown to prevent the timely decatenation of yeast minichromosomes (Charbin et al., 2014). Early in vitro studies demonstrated that condensin overwinds DNA generating positive supercoiling in the presence of type IB topoisomerases (Bazett-Jones et al., 2002; Kimura and Hirano, 1997), and this activity was recently described in vivo on yeast minichromosomes (Baxter et al., 2011). Moreover, TopoIIα (one of the eukaryotic type IIA topoisomerases) shows a bias towards decatenation on catenated plasmids that are positively supercoiled but not on negatively supercoiled substrates (Baxter et al., 2011), raising the possibility that condensin-dependent overwinding indirectly promotes decatenation by Top2 through alteration of substrate topology (Baxter and Aragón, 2012). In mammals, TopoIIα and condensin are present on chromosome axes (Maeshima and Laemmli, 2003), and recent data from chicken DT40 cell lines demonstrated that inactivation of condensin function prevents TopoIIα localization (Samejima et al., 2012).

Sister chromatid intertwines (SCIs) persist on cohesin sites until biorientation on mitotic spindles takes place (Farcas et al., 2011). Direct visualization of SCIs on yeast minichromosomes using sucrose gradient fractionation and southern analysis demonstrated that SCIs are present on minichromosomes in a metaphase arrest without spindles (nocodazole arrests) but they disappear as chromosomes become bioriented in a metaphase arrest with spindles (cdc20-depletion arrests) (Farcas et al., 2011). Coincidentally, this mirrors the overwinding activity observed for condensin, which is absent in nocodazole arrests but present in cdc20-depletion arrests (Baxter et al., 2011).

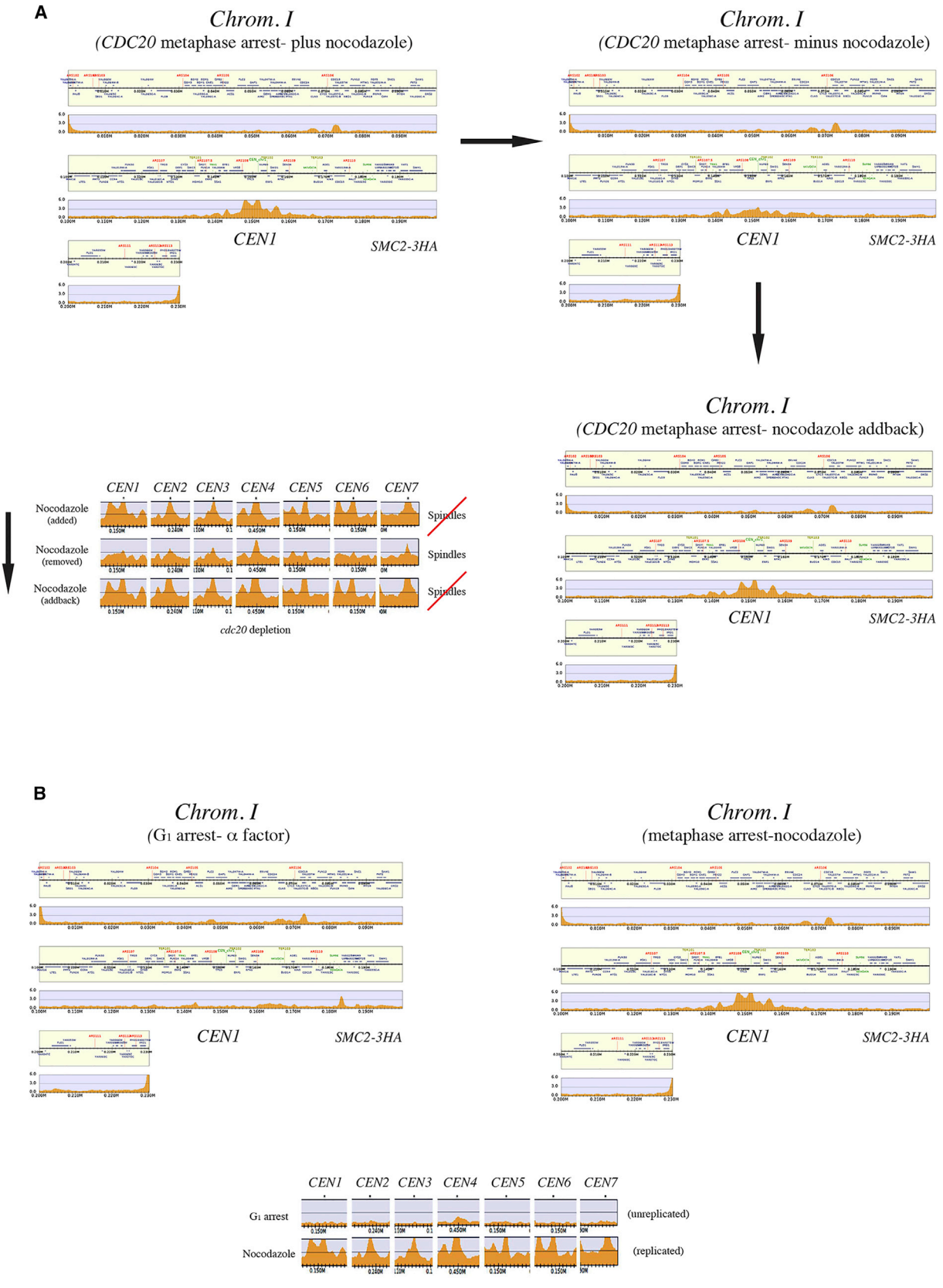

(legend on next page)

During early yeast mitosis (metaphase) condensin localizes to centromeres (D'Ambrosio et al., 2008; Verzijlbergen et al., 2014) and plays specific roles in sensing kinetochore tension (Yong-Gonzalez et al., 2007) and biorientation (Verzijlbergen et al., 2014). In late mitosis (anaphase), condensin subunits become hyperphosphorylated by Cdc5 polo-kinase (St-Pierre et al., 2009), a modification shown to enhance condensin's overwinding activity in vitro (St-Pierre et al., 2009). Importantly, this anaphase role of condensin has been linked to a late-condensation step during chromosome segregation (Lavoie et al., 2004; Machín et al., 2005) necessary to remove residual cohesin complexes (Renshaw et al., 2010) and prevent chromosome breakage (Cuylen et al., 2013).

Here, we show that condensin binds to centromere regions only after DNA replication and it is transiently relocalized to chromosome arms during yeast anaphase. We also characterize the requirements and consequences of condensin's anaphase relocalization.

RESULTS

Chromosome Biorientation Promotes Reduced Condensin Binding at Centromeres

Previous work has demonstrated that condensin is enriched at the ribosomal gene array and centromeres sequences in metaphase arrests mediated by nocodazole, where cells lack mitotic spindles (D'Ambrosio et al., 2008; Verzijlbergen et al., 2014). Condensin-dependent DNA overwinding is also absent in nocodazole-arrested cells (Baxter et al., 2011). Therefore, biorientation on the spindles not only requires condensin (Verzijlbergen et al., 2014), but it also triggers condensin-dependent overwinding on minichromosomes (Baxter et al., 2011). We set out to investigate whether the centromeric localization of condensin in nocodazole-arrested cells is altered upon chromosome biorientation. To this aim, we compared centromeric localization of Smc2 by chromatin immunoprecipitation sequencing (ChIP-seq) analysis on cells arrested in metaphase by depletion of the APC activator cdc20 in the presence or absence of mitotic spindles (Figure 1A). Cdc20-depleted cells were first arrested in metaphase in the presence of nocodazole (where the spindles are absent) (Figure 1A; *CDC20* arrests-plus nocodazole). As previously described, Smc2 was enriched at centromere cores and pericentromeric regions (D'Ambrosio et al., 2008; Verzijlbergen et al., 2014) (Figure 1A). Next, nocodazole was removed from the culture to allow spindle formation in the cdc20-depleted cells. This led to a significant reduction in Smc2 binding around centromeres (Figure 1A; *CDC20* arrests—minus nocodazole) suggesting that condensin association is reduced when chromosomes achieve biorientation. To test whether lack of chromosome biorientation is responsible for the binding of condensin around centromeres, we added new nocodazole to Cdc20-depleted cells (Figure 1A; *CDC20* arrests—nocodazole add-back). High Smc2 binding around centromeres was re-established in these cells (Figure 1A). In contrast to metaphase arrests treated with nocodazole, Smc2 enrichment around centromeres was completely abolished in G1-arrested cells (Figure 1B). We were surprised by this result because previous studies reported unaltered chromosomal binding of condensin to centromeres throughout the cell cycle (D'Ambrosio et al., 2008). To confirm our results, we decided to use ChIP-qPCR analysis at various time points following a synchronized culture release from a G1 arrest (Figure 2A). We used two primer pairs covering the regions around the centromere of chromosome 4 and three locations in the long chromosome arm at different distances from the centromere (15, 50, and 100 kb away) (Figure 2A). Consistent with our ChIP-seq data, we observed that Smc2 binding occurred at centromere regions only after genome replication (Figure 2A). From these results, we conclude that condensin binds to replicated chromosomes mainly around centromere regions (Figure 1; Data S1, S2, S3, and S4).

Condensin Relocalizes to Chromosome Arms

During our ChIP-seq analysis, we observed the localization of condensin to centromere regions in the presence of nocodazole but not in cells arrested in metaphase by Cdc20 depletion (Figure 1A), suggesting that biorientation causes condensin dissociation. We decided to further investigate this using ChIP-qPCR analysis on various chromosome regions around the vicinity of the *CEN* sequence of chromosome 4. We arrested cdc20-depleted cells in metaphase in the presence of nocodazole, removed the spindle poison, and took samples for analysis at various time points after nocodazole removal. Cytological analysis of mitotic spindles confirmed their formation after nocodazole removal (data not shown). Analysis of Smc2 localization by ChIP-qPCR revealed an increase in binding to the core centromere (*CEN4-0*) upon nocodazole removal (10 min) (Figure 2B) followed by a steady decrease overtime leading to significantly lower levels to those observed in the previous nocodazole arrests (Figure 2B). This is consistent with our observations using ChIP-seq, where condensin localization decreased significantly after 120 min of nocodazole removal (Figure 1A). Next, we wondered whether the dissociation of condensin from centromeres (Figure 2B) leads to relocalization of the complex to other chromosomal regions. To investigate this, we extended our analysis to chromosomal regions 15, 50, and 100 kb away from *CEN4* (Figure 2C). As centromere binding of Smc2 decreased (Figure 2C; from 20 min

Figure 1. Chromosome Biorientation Promotes Reduced Condensin Binding at Centromeres

(A) Association of condensin subunit Smc2 by ChIP-seq analysis to chromosomes in metaphase arrested cells in the presence and absence of mitotic spindles. *cdc20-td SMC2-3HA* cells were arrested in metaphase with nocodazole under Cdc20 depleting conditions (*CDC20* metaphase arrest-plus nocodazole). After the arrest, nocodazole was removed and samples collected at 120 min (*CDC20* metaphase arrest-minus nocodazole). Finally, nocodazole was added back and samples collected after 120 min (*CDC20* metaphase arrest- nocodazole addback). Note that Smc2 centromere localization is inversely correlated to the presence of spindles.

(B) Cells as in (A) were synchronized in G1 and released into the cell cycle in the presence of nocodazole. Samples were taken for analysis at the G1 block and 120 min after release when cells reached metaphase arrest. Note that Smc2 centromeric localization is absent in cells arrested in G1.

See also Data S1, S2, S3, and S4.

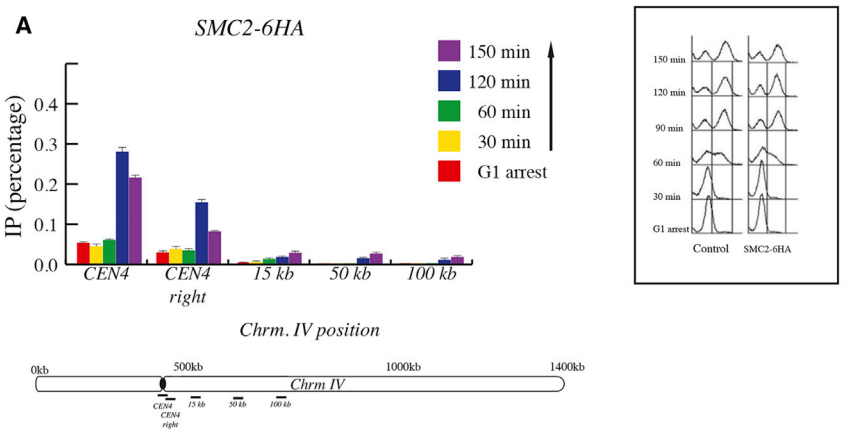

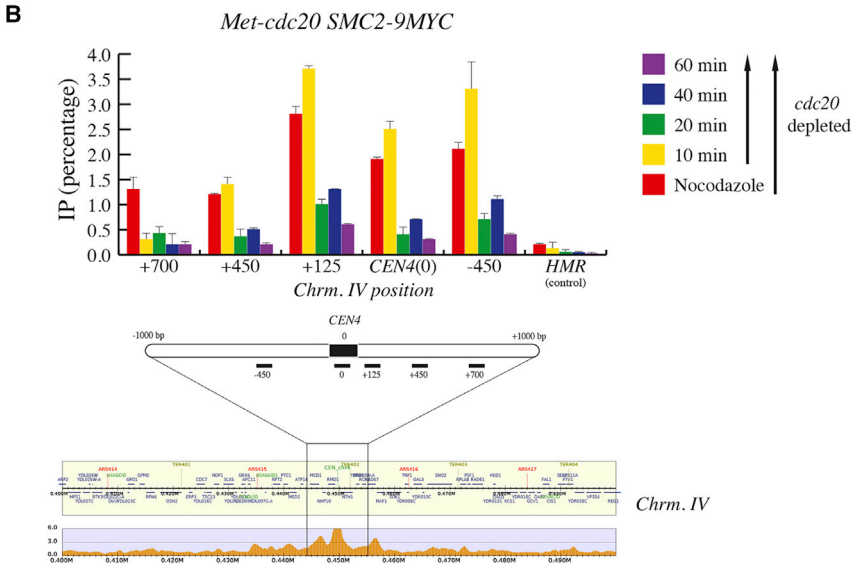

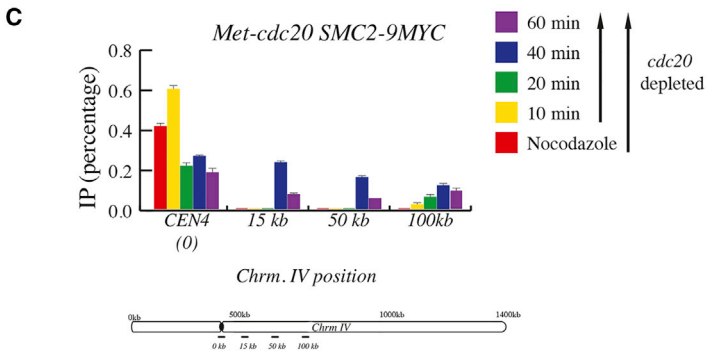

Figure 2. Condensin Localizes to the Chromosome upon Chromosome Biorientation

(A) *SMC2-6HA* cells were synchronized in G1 and released into the cell cycle. Samples were taken at the indicated time points and processed for ChIP-qPCR analysis. Graphs show the mean ± SD.

(B) *Met-CDC20 SMC2-9MYC* cells were arrested in metaphase with nocodazole under Cdc20 depleting conditions. Cells were transferred to new media lacking nocodazole at 37°C and samples collected for ChIP-qPCR analysis at the indicated times. Graphs show the mean ± SD.

(C) Cells were treated as in (B). Chromosomal association at selected positions was determined by ChIP-qPCR. Graphs show the mean ± SD.

onward), binding on arm regions increased following nocodazole removal (Figure 2C; 40 and 60 min). These results demonstrate that, following biorientation of sister chromatids on the mitotic spindles, condensin binding around centromeres is decreased while its binding at chromosome arm regions increases.

Condensin Relocalization Depends on Polo-Kinase Cdc5 and Correlates with Its Activity Promoting DNA Overwinding

Condensin activity during mitosis is regulated by several kinases, including Aurora B Ipl1 (Lavoie et al., 2004), Cdk1 (Kimura et al., 1998; Robellet et al., 2015; Sutani et al., 1999), and polo kinase Cdc5 (St-Pierre et al., 2009). Importantly, Cdc5 phosphorylation affects several subunits of condensin and causes condensin to overwind DNA in vitro (St-Pierre et al., 2009). Moreover, Cdc5 is necessary for anaphase-chromosome condensation and segregation (St-Pierre et al., 2009). First, we decided to confirm that Cdc5 is required for condensin's DNA overwinding activity in vivo. Mitotic overwinding by condensin is associated with a change in electrophoretic mobility of yeast minichromosomes in the absence of Top2 activity (Baxter et al., 2011). The shift in gel mobility is caused by a transition from catenated dimers that are negatively supercoiled (CatC) to catenated dimers that are positively supercoiled (CatC*) (Baxter et al., 2011). To test a potential requirement for Cdc5 in condensin-dependent overwinding, we compared minichromosome migration in cells released from G1 in the absence of Top2 (*top2-td*) or both Top2 and Cdc5 (*cdc20-td cdc5-1*) (Figure 3A). CatC* (overwound catenanes- positively supercoiled) were only observed in cells with Cdc5 activity but not in *cdc5-1* samples (Figure 3A) demonstrating that this kinase is indeed required for DNA overwinding. A similar analysis in cells lacking Aurora B demonstrated that this kinase also contributes to DNA overwinding (Figure 3A). Inactivation of Ipl1 led to defects in the formation of CatC* (overwound catenanes—positively

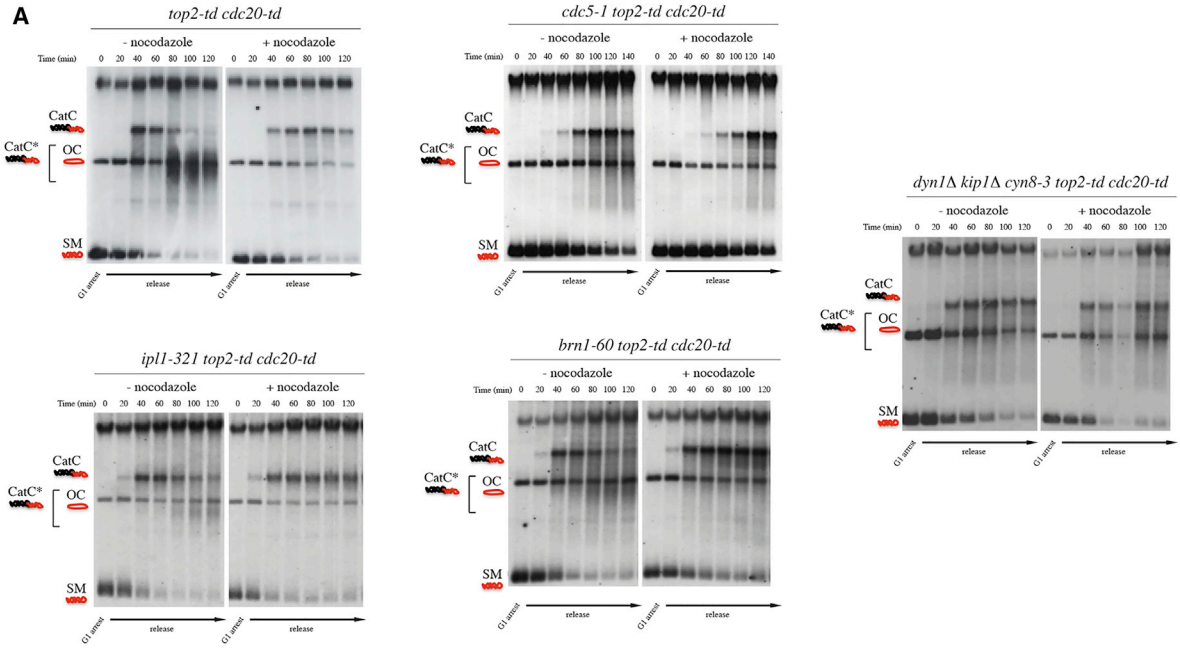

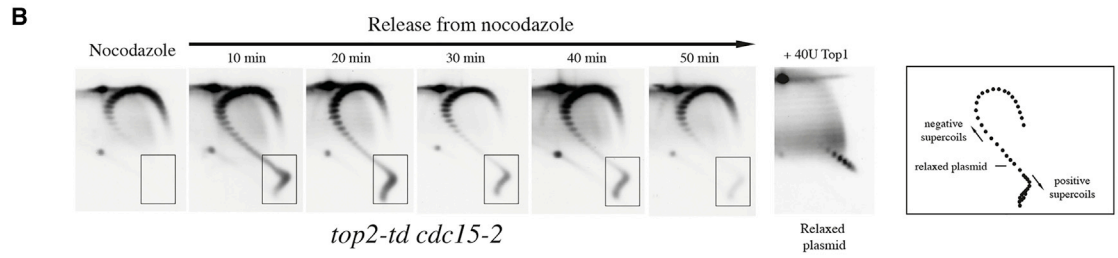

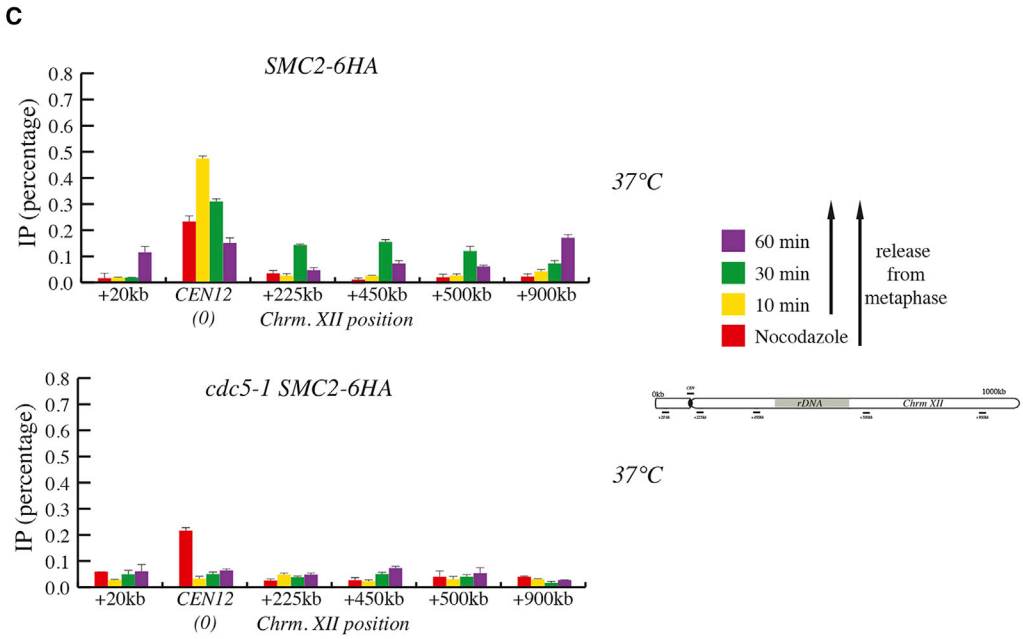

(legend on next page)

supercoiled) similar to those observed in conditional mutants of the condensin subunit Brn1 (Figure 3A). This is consistent with previous studies linking Ipl1 function to condensin phosphorylation (St-Pierre et al., 2009). In addition, we found that tension across bioriented sister kinetochores is also necessary for overwinding, as we did not detect CatC* formation when spindle motors, Dyn1, Kip1, and Cyn8-3 were inactivated (Figure 3A), despite the fact that kinetochore-spindle attachments are intact in these cells (Saunders et al., 1995). Next, we investigated whether condensin overwinding occurs normally during anaphase. We looked for the formation of positively supercoiled plasmid topoisomers during a release from metaphase (nocodazole block) to telophase (mediated by *cdc15-2* conditional mutant) using 2D chloroquine gels to reveal the supercoiling distribution of the monomer plasmids (Figure 3B). We observed the formation of positively supercoiled monomers as the cells proceeded through anaphase (Figure 3B), demonstrating that condensin overwinding activity occurs during anaphase. Next, we decided to investigate the potential correlation between condensin overwinding and the relocalization from centromeres to chromosome arms we had observed since both events occur in anaphase. To this aim, we tested whether in the absence of Cdc5 activity, which is required for condensin-mediated overwinding (Figure 3A), condensin relocalization to chromosome arms occurs. We used the conditional allele *cdc5-1* and looked at the localization of Smc2 to the arms of chromosome 12 during a metaphase release in the presence and absence of Cdc5 activity. Similar to what we had observed for chromosome 4 in cdc20-depleted conditions (Figure 2C), Smc2 showed enrichment at centromeres upon nocodazole removal followed by binding to chromosome 12 arms regions during anaphase when Cdc5 activity was present (Figure 3C). In contrast, binding to arm regions was not observed in the absence of Cdc5 (Figure 3C). This result demonstrates that Cdc5 is essential for the relocalization of condensin to arm regions during anaphase and establishes a temporal correlation between condensin-dependent overwinding and its localization to chromosome arm regions.

Condensin Behavior during Anaphase Involves a Higher Binding Rate on DNA

Photobleaching analysis of fluorescently labeled condensin subunits has shown that the binding of the complex (condensin I) to mammalian chromosomes is highly dynamic (Gerlich et al., 2006). Our results demonstrate that Smc2 is differentially enriched at centromeres in the presence of nocodazole and on chromosome arms during anaphase in a Cdc5-dependent manner (Figure 3C), we therefore wondered whether differences in dynamic binding of condensin exist before and after activation by Cdc5. To investigate this, we used cross-linking kinetic (CLK) analysis (Poorey et al., 2013) of Smc2 to the centromere of chromosome 4 (*CEN4*). This approach uses time-dependence of formaldehyde crosslinking to extract on- and off-rates for chromatin binding in vivo (Poorey et al., 2013). We compared *CEN4* ChIP dataset, spanning a range of crosslinking times, between cells arrested in nocodazole and cells just released from nocodazole (at 10 min of release), when increased binding to centromeres was observed in a Cdc5-dependent manner (Figure 3C). The CLK profiles observed for Smc2 best fitted those described for transcription factors with a fast on and off rate and low occupancy (Figure 4A) (Poorey et al., 2013). This is in good agreement with the highly dynamic behavior reported for condensin on mammalian chromosomes (Gerlich et al., 2006), flies (Oliveira et al., 2007), and yeast (Robellet et al., 2015). In addition, the binding rate for Smc2 was increased 2-fold in cells just released from nocodazole (Figure 4A; 10 min after nocodazole removal—post spindles). We conclude from these results that yeast condensin, like mammalian condensin I, is highly dynamic and binds faster after Cdc5-dependent activation in anaphase.

Condensin Promotes Recruitment of Top2 to Anaphase Chromosomes

Recent work demonstrated that inactivation of condensin in chicken DT40 cell lines prevents TopoIIα localization to mitotic chromosomes (Samejima et al., 2012). Similarly, inactivation of yeast condensin has been shown to prevent the timely decatenation of minichromosomes (Charbin et al., 2014). Moreover, condensin mutants insensitive to Cdc5 phosphorylation show condensation/segregation defects (St-Pierre et al., 2009). We therefore set out to investigate whether the Cdc5-dependent relocalization of condensin to chromosome arms is important for Top2 recruitment to chromosomes. To this aim, we initially tested whether Top2 could be detected on chromosome arms during a release from nocodazole. We used ChIP-qPCR to several regions covering the long arm of chromosome 12 in cells expressing Top2 tagged with HA epitopes. We detected Top2

Figure 3. Condensin-Mediated DNA Supercoiling and Localization to Chromosome Arms Temporally Overlap during Anaphase and Require Polo Kinase

(A) *Cdc20-td top2-td*, *cdc20-td top2-td cdc5-1*, *cdc20-td top2-td ipl1-321*, *cdc20-td top2-td brn1-60*, and *cdc20-td top2-td dyn1*Δ *kip1*Δ *cyn8-3* strains bearing a circular centromeric minichromosome (pRS316) were synchronized in G1, split in two, and released into the cell cycle under conditions of Cdc20 and Top2 depletion at 37°C. Nocodazole was added to one of the samples. DNA was resolved in agarose gels and probed for the circular minichromosome. Electrophoretic mobility of monomers (OCm, relaxed monomer; Lm, linear monomer; CCCm, supercoiled monomer) is indicated. Dimeric forms CatC type catenanes (negatively supercoiled) and CatC* type catenanes—(positively supercoiled) are indicated.

(B) A *top2-td cdc15-2* strain carrying a minichromosome (pRS316) was synchronously arrested in mitosis using nocodazole to prevent formation of mitotic spindles. Top2 protein was then degraded before washing off the nocodazole to allow mitotic spindles to form and cells were allowed to proceed to a telophase arrest at 37°C mediated by *cdc15-2*. DNA was analyzed in 2D chloroquine gels to reveal the supercoiling distribution of the monomer plasmids. To assign the mobility of topoisomers (as positive or negative) we treated minichromosomes with eukaryotic topoisomerase I and run the fully relaxed plasmids under the same gel conditions. A cartoon representation of how the plasmid distribution relates to supercoiling status is shown (right). OC, open circles; SM, supercoiled monomer; CatC, type C catenane negatively supercoiled; CatC*, type C catenane positively supercoiled.

(C) *SMC2-6HA* and *cdc5-1 SMC2-6HA* cells were synchronized in G1 and released into the cell cycle in the presence of nocodazole. Following metaphase arrest, cells were transferred to new media lacking nocodazole at 37°C and samples were collected at the indicated time points. Association to chromosome 12 was determined by ChIP-qPCR. Graphs show the mean ± SD.

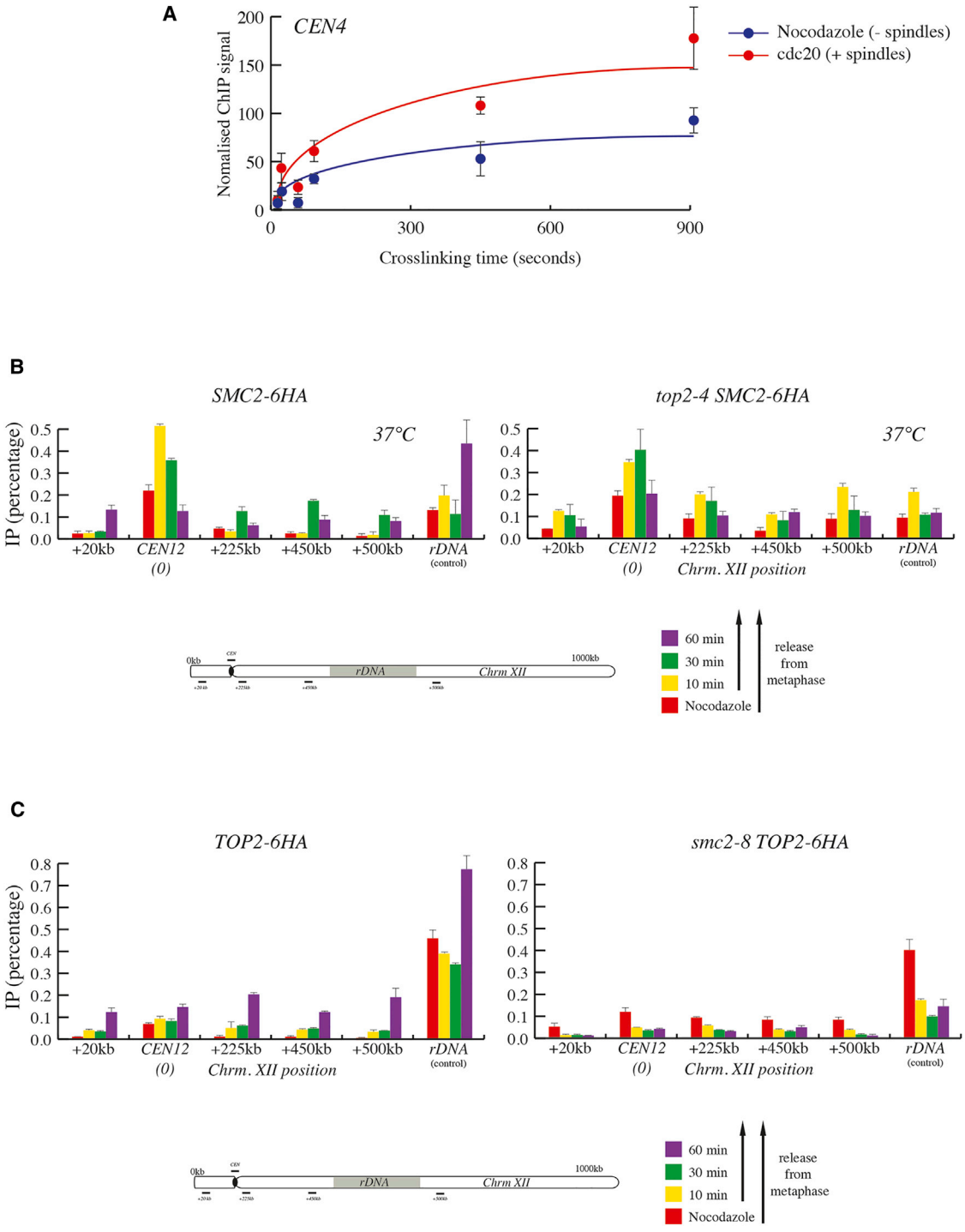

Figure 4. Condensin Localization in Anaphase Involves a Higher Binding Rate on DNA and Promotes Top2 Binding to Chromosome Arms

(A) CLK analysis for *SMC2-3HA* binding to *CEN4* in cells arrested in nocodazole (−spindles; blue) or released to a cdc20 block (+spindles; red). Conditions were as in Figure 2B. Smc2 binding to *CEN4* was determined by ChIP-qPCR for each crosslinking time. Data and fits are shown. Graphs show the mean ± SD.

(B) *SMC2-6HA* and *top2-4 SMC2-6HA* cells were synchronized in G1 and released into the cell cycle in the presence of nocodazole. Following metaphase arrest, cells were transferred to new media lacking nocodazole at 37°C and samples were collected at the indicated time points. Chromosomal association at selected positions was determined by ChIP-qPCR. Graphs show the mean ± SD.

(C) *TOP2-6HA* and *smc2-8 TOP2-6HA* cells were treated and analyzed as in (B). Graphs show the mean ± SD.

recruitment to chromosome arms during late time points of the release (Figure 4C; 60 min), similar to what we had observed for Smc2 (Figure 3C). Unlike Smc2, we did not detect an increase in Top2 binding to core centromere regions upon nocodazole removal (Figure 4C). Next, we investigated whether Top2 binding to chromosomes required condensin. We used the conditional allele *smc2-8* to inactivate Smc2 in a nocodazole release. We did not detect any Top2 enrichment at late time points in *smc2-8* samples (Figure 4C) demonstrating that Top2 requires condensin function for localization to chromosome arms. The functional relation between Top2 and condensin prompted us to further investigate whether inactivation of Top2 also affected condensin localization to chromosomes arms. Time course analysis of Smc2 localization in metaphase releases lacking Top2 function (using the conditional allele, *top2-4*) revealed an accumulation of Smc2 binding on chromosome arms (Figure 4B). These results demonstrate that condensin recruitment does not depend on Top2; however, the persistence in condensin binding observed in *top2-4* mutants suggests that the transient localization of condensin to chromosome arms during anaphase is affected by Top2 activity.

DISCUSSION

Our work provides insights into the coordination of condensin and topoisomerase II functions during chromosome segregation. Although a role for condensin in anaphase condensation had been proposed earlier (Cuylen et al., 2013; Lavoie et al., 2004; Machín et al., 2005; Renshaw et al., 2010; St-Pierre et al., 2009), neither its detailed regulation and activation nor its consequences had been fully elucidated. First, we have demonstrated that condensin binding around centromere regions occurs after DNA replication. Then, upon bipolar attachment to the spindles, condensin activation by Cdc5 (St-Pierre et al., 2009) causes it to become localized to chromosome arms with increased dynamics. Moreover, this step in condensin activation coincides with the time of the DNA overwinding activity described earlier (Baxter et al., 2011; Kimura and Hirano, 1997) and the recruitment of Top2 to anaphase chromosomes as they are being segregated. We previously proposed a model where the role of topoisomerases in mitotic chromosome architecture was to respond to the enzymatic activity of condensin by relaxing condensin-dependent supercoiling (caused by condensin's overwinding activity) and in addition to such role in supercoil relaxation to remove any remaining chromosomal intertwinings (SCI) (Baxter and Aragón, 2012). On the other hand, condensin's molecular function was to promote overwinding-mediated compaction of the DNA that would attract Top2. In such a model, varying the rates of condensin overwinding or Top2 relaxation activities could lead to distinct changes in the shape and mechanical properties of chromosomes (Baxter and Aragón, 2012). Interestingly, recent studies looking at mammalian mitotic chromosome structure in the absence of condensin and topoisomerase IIα function demonstrated opposing activities for condensin and topoisomerase IIα (Samejima et al., 2012) consistent with this model.

Our data suggest that at the anaphase onset, condensin-dependent overwinding is activated and the rate of condensin association with DNA changes, as we detected a 2-fold increase in binding rates (Figure 4A). We show that Top2 binding responds to condensin's overwinding activity by being enriched on chromosome arms. Furthermore, when cellular supercoil relaxation activities are decreased in the absence of Top2 (note that Top1 can partially compensate relaxation), condensin binding as predicted in this model is altered (Figure 4B). Therefore, our results are fully consistent with a model where the rates of condensin and Top2 molecular activities are coordinated to shape condensed chromosomes and to remove intertwinings in the replicated genome.

EXPERIMENTAL PROCEDURES

Yeast strains used in this study are fully listed in Table S1. Detailed experimental procedures are provided in the Supplemental Experimental Procedures. Specific cell growth and synchronization conditions used for each experiment are described in the corresponding figure legend. Analysis of mini-chromosome topology was done as described earlier (Baxter et al., 2011) with minor changes indicated in the Supplemental Experimental Procedures.

For ChIP-seq analysis, reads were aligned to the *Saccharomyces cerevisiae* genome sequence using Bowtie (Langmead et al., 2009). Mapping results were processed and converted to genome-wide protein distribution profiles (ChIP-seq profiles) using parse2wig and DROMPA software as described (Sutani et al., 2015).

ChIP-qPCR conditions are described in detail in the Supplemental Experimental Procedures. CLK analysis was done as in Poorey et al. (2013). To eliminate non-specific enrichment due to transcription in our ChIP analysis, as it has been recently demonstrated (Teytelman et al., 2013), we used tagged and untagged strains and compared the enrichment in tagged strains relative to the untagged controls. First, ChIP-qPCR experiments signals obtained for both tagged and isogenic untagged strains were each normalized to their respective input samples. Then signals for each primer pair from untagged strains were subtracted from those obtained for the tagged samples. The results obtained are presented as the percentages of the recovery over the input.

SUPPLEMENTAL INFORMATION

Supplemental Information includes Supplemental Experimental Procedures, two tables, and four data files and can be found with this article online at http://dx.doi.org/10.1016/j.celrep.2015.11.041.

ACKNOWLEDGMENTS

We would like to thank present and former members of the L.A. laboratory for discussions and critical reading of the manuscript. This work was funded by the Intramural Research Programme of the Medical Research Council UK (J.L.) and a Wellcome Trust Award (100955-"Functional dissection of mitotic chromatin") to L.A. (N.S. and R.T.) as well as a Grant-in-Aid for Scientific Research on Innovative Areas "Chromosome Orchestration System" from MEXT to K.S.

Received: July 14, 2015
Revised: September 8, 2015
Accepted: November 11, 2015
Published: December 10, 2015

REFERENCES

Baxter, J., and Aragón, L. (2012). A model for chromosome condensation based on the interplay between condensin and topoisomerase II. Trends Genet. *28*, 110–117.

Baxter, J., Sen, N., Martínez, V.L., De Carandini, M.E., Schvartzman, J.B., Diffley, J.F., and Aragón, L. (2011). Positive supercoiling of mitotic DNA drives decatenation by topoisomerase II in eukaryotes. Science *331*, 1328–1332.

Bazett-Jones, D.P., Kimura, K., and Hirano, T. (2002). Efficient supercoiling of DNA by a single condensin complex as revealed by electron spectroscopic imaging. Mol. Cell *9*, 1183–1190.

Charbin, A., Bouchoux, C., and Uhlmann, F. (2014). Condensin aids sister chromatid decatenation by topoisomerase II. Nucleic Acids Res. *42*, 340–348.

Cuylen, S., Metz, J., Hruby, A., and Haering, C.H. (2013). Entrapment of chromosomes by condensin rings prevents their breakage during cytokinesis. Dev. Cell *27*, 469–478.

D'Ambrosio, C., Schmidt, C.K., Katou, Y., Kelly, G., Itoh, T., Shirahige, K., and Uhlmann, F. (2008). Identification of cis-acting sites for condensin loading onto budding yeast chromosomes. Genes Dev. *22*, 2215–2227.

Farcas, A.M., Uluocak, P., Helmhart, W., and Nasmyth, K. (2011). Cohesin's concatenation of sister DNAs maintains their intertwining. Mol. Cell *44*, 97–107.

Freeman, L., Aragon-Alcaide, L., and Strunnikov, A. (2000). The condensin complex governs chromosome condensation and mitotic transmission of rDNA. J. Cell Biol. *149*, 811–824.

Gerlich, D., Hirota, T., Koch, B., Peters, J.M., and Ellenberg, J. (2006). Condensin I stabilizes chromosomes mechanically through a dynamic interaction in live cells. Curr. Biol. *16*, 333–344.

Hirano, T. (2005). Condensins: organizing and segregating the genome. Curr. Biol. *15*, R265–R275.

Holm, C., Goto, T., Wang, J.C., and Botstein, D. (1985). DNA topoisomerase II is required at the time of mitosis in yeast. Cell *41*, 553–563.

Kimura, K., and Hirano, T. (1997). ATP-dependent positive supercoiling of DNA by 13S condensin: a biochemical implication for chromosome condensation. Cell *90*, 625–634.

Kimura, K., Hirano, M., Kobayashi, R., and Hirano, T. (1998). Phosphorylation and activation of 13S condensin by Cdc2 in vitro. Science *282*, 487–490.

Koshland, D., and Strunnikov, A. (1996). Mitotic chromosome condensation. Annu. Rev. Cell Dev. Biol. *12*, 305–333.

Langmead, B., Trapnell, C., Pop, M., and Salzberg, S.L. (2009). Ultrafast and memory-efficient alignment of short DNA sequences to the human genome. Genome Biol. *10*, R25.

Lavoie, B.D., Hogan, E., and Koshland, D. (2004). In vivo requirements for rDNA chromosome condensation reveal two cell-cycle-regulated pathways for mitotic chromosome folding. Genes Dev. *18*, 76–87.

Machín, F., Torres-Rosell, J., Jarmuz, A., and Aragón, L. (2005). Spindle-independent condensation-mediated segregation of yeast ribosomal DNA in late anaphase. J. Cell Biol. *168*, 209–219.

Maeshima, K., and Laemmli, U.K. (2003). A two-step scaffolding model for mitotic chromosome assembly. Dev. Cell *4*, 467–480.

Nasmyth, K. (2001). Disseminating the genome: joining, resolving, and separating sister chromatids during mitosis and meiosis. Annu. Rev. Genet. *35*, 673–745.

Oliveira, R.A., Heidmann, S., and Sunkel, C.E. (2007). Condensin I binds chromatin early in prophase and displays a highly dynamic association with Drosophila mitotic chromosomes. Chromosoma *116*, 259–274.

Ono, T., Losada, A., Hirano, M., Myers, M.P., Neuwald, A.F., and Hirano, T. (2003). Differential contributions of condensin I and condensin II to mitotic chromosome architecture in vertebrate cells. Cell *115*, 109–121.

Poorey, K., Viswanathan, R., Carver, M.N., Karpova, T.S., Cirimotich, S.M., McNally, J.G., Bekiranov, S., and Auble, D.T. (2013). Measuring chromatin interaction dynamics on the second time scale at single-copy genes. Science *342*, 369–372.

Renshaw, M.J., Ward, J.J., Kanemaki, M., Natsume, K., Nédélec, F.J., and Tanaka, T.U. (2010). Condensins promote chromosome recoiling during early anaphase to complete sister chromatid separation. Dev. Cell *19*, 232–244.

Robellet, X., Thattikota, Y., Wang, F., Wee, T.L., Pascariu, M., Shankar, S., Bonneil, É., Brown, C.M., and D'Amours, D. (2015). A high-sensitivity phospho-switch triggered by Cdk1 governs chromosome morphogenesis during cell division. Genes Dev. *29*, 426–439.

Saka, Y., Sutani, T., Yamashita, Y., Saitoh, S., Takeuchi, M., Nakaseko, Y., and Yanagida, M. (1994). Fission yeast cut3 and cut14, members of a ubiquitous protein family, are required for chromosome condensation and segregation in mitosis. EMBO J. *13*, 4938–4952.

Samejima, K., Samejima, I., Vagnarelli, P., Ogawa, H., Vargiu, G., Kelly, D.A., de Lima Alves, F., Kerr, A., Green, L.C., Hudson, D.F., et al. (2012). Mitotic chromosomes are compacted laterally by KIF4 and condensin and axially by topoisomerase IIα. J. Cell Biol. *199*, 755–770.

Saunders, W.S., Koshland, D., Eshel, D., Gibbons, I.R., and Hoyt, M.A. (1995). Saccharomyces cerevisiae kinesin- and dynein-related proteins required for anaphase chromosome segregation. J. Cell Biol. *128*, 617–624.

Shintomi, K., and Hirano, T. (2011). The relative ratio of condensin I to II determines chromosome shapes. Genes Dev. *25*, 1464–1469.

St-Pierre, J., Douziech, M., Bazile, F., Pascariu, M., Bonneil, E., Sauvé, V., Ratsima, H., and D'Amours, D. (2009). Polo kinase regulates mitotic chromosome condensation by hyperactivation of condensin DNA supercoiling activity. Mol. Cell *34*, 416–426.

Sundin, O., and Varshavsky, A. (1980). Terminal stages of SV40 DNA replication proceed via multiply intertwined catenated dimers. Cell *21*, 103–114.

Sutani, T., Yuasa, T., Tomonaga, T., Dohmae, N., Takio, K., and Yanagida, M. (1999). Fission yeast condensin complex: essential roles of non-SMC subunits for condensation and Cdc2 phosphorylation of Cut3/SMC4. Genes Dev. *13*, 2271–2283.

Sutani, T., Sakata, T., Nakato, R., Masuda, K., Ishibashi, M., Yamashita, D., Suzuki, Y., Hirano, T., Bando, M., and Shirahige, K. (2015). Condensin targets and reduces unwound DNA structure associated with transcription in mitotic chromosome condensation. Nat. Commun. *6*, 7815.

Teytelman, L., Thurtle, D.M., Rine, J., and van Oudenaarden, A. (2013). Highly expressed loci are vulnerable to misleading ChIP localization of multiple unrelated proteins. Proc. Natl. Acad. Sci. USA *110*, 18602–18607.

Uemura, T., Ohkura, H., Adachi, Y., Morino, K., Shiozaki, K., and Yanagida, M. (1987). DNA topoisomerase II is required for condensation and separation of mitotic chromosomes in S. pombe. Cell *50*, 917–925.

Verzijlbergen, K.F., Nerusheva, O.O., Kelly, D., Kerr, A., Clift, D., de Lima Alves, F., Rappsilber, J., and Marston, A.L. (2014). Shugoshin biases chromosomes for biorientation through condensin recruitment to the pericentromere. eLife *3*, e01374.

Wang, J.C. (2002). Cellular roles of DNA topoisomerases: a molecular perspective. Nat. Rev. Mol. Cell Biol. *3*, 430–440.

Yong-Gonzalez, V., Wang, B.D., Butylin, P., Ouspenski, I., and Strunnikov, A. (2007). Condensin function at centromere chromatin facilitates proper kinetochore tension and ensures correct mitotic segregation of sister chromatids. Genes Cells *12*, 1075–1090.

Cell Reports

Supplemental Information

Condensin Relocalization from Centromeres to Chromosome Arms Promotes Top2 Recruitment during Anaphase

Joanne Leonard, Nicholas Sen, Raul Torres, Takashi Sutani, Adam Jarmuz, Katsuhiko Shirahige, and Luis Aragon

Supplementary materials

Title: Condensin relocalisation from centromeres to chromosome arms promotes Top2 recruitment during anaphase

Authors: Joanne Leonard, Nicholas Sen, Raul Torres, Takashi Sutani1, Adam Jarmuz, Katsuhiko Shirahige & Luis Aragon.

Experimental Procedures

Strains and Growth conditions

Yeast strains bearing the minichromosome plasmid (pRS316-URA) were grown in synthetic media lacking uracil. For nocodazole arrests we used 15μg/ml nocodazole incubations for 3 hours. Strains bearing the temperature sensitive degron cdc20-td or top2-td cells were grown exponentially. These cultures were diluted to OD600= 0.25 in YEP media supplemented with 2% Raffinose (YEPRaff) and allowed to grow for 8 hours, before being diluted to OD600= 0.05 in YEPRaff and allowed to grow overnight. Exponentially growing cultures on day three were subsequently diluted to OD600= 0.25 and allowed to grow for 3 hours at 25°C. Temperature sensitive alleles were then triggered by the addition of Galactose to 2% final concentration. Doxycycline was added to 50μg/ml final concentration, and a temperature shift to 37°C was introduced. Where a release from an early metaphase arrest to a cdc20td-mediated arrest was required, cells were first arrested in nocodazole, before the nocodazole was washed off and pellets resuspended in YEP2%Raff, 2%Gal, 50μg/ml Doxycycline, at 37°C. Cells remained in these conditions for 2 hours to ensure

passage to a cdc20td-mediated arrest was attained. For nocodazole wash off experiments cells were initially synchronised in alpha factor in YP media and released to a metaphase block using nocodazole at 25°C. Following 90 minutes incubation the culture was examined for mitotic block morphology (only arrests with >90% budding were used). For strains bearing conditional alleles the cultures were shifted to 37°C for 1 hour while in nocodazole. Nocodazole was then washed off and the cells incubated in YP media with cell samples taken at the indicated times.

Genomic DNA Preparation

Cells were harvested at 4000rpm and pellets were washed with ice cold H_2O and stored at -80°C. Frozen pellets were re-suspended in lysis buffer (50mM Tris-HCl pH 8.0, 100mM NaCl, 10mM EDTA, 1%SDS) and the cell wall removed by incubation with 80 units/ml Lyticase (Sigma) and 1% β-mercaptoethanol (Sigma) at 37°C for 5 min. DNA was then extracted by phenol/chloroform/isoamylalcohol (25:24:1) and the aqueous layer removed using phase lock tubes (5 Prime). For agarose gel analysis DNA was precipitated with 2 volumes of 100% ethanol and washed with 70 % ethanol before being re-solubilized in 10mM Tris pH8.0.

Agarose Gel analysis

DNA was resolved by 1D electrophoresis in 0.8% agarose (Megasieve, Flowgen) 0.5X TBE gels. Gels were run for 24 hours at 2.5V/cm. Plasmid pRS316 was detected by probing with DNA amplified from sequences of pRS316 including the URA3 sequences. For two dimensional neutral-neutral gel electrophoresis with chloroquine, the first dimension was run in 0.4% agarose (1.4 g of Mega Sieve agarose in 350 ml 1x TBE buffer) with 0.5 μg/ml chloroquine added. A DNA ladder (Promega) and a guide plasmid from *E. coli* were loaded and run at 30 V for 40 hours at room

temperature in 1x TBE buffer with 0.5 μg/ml chloroquine. The ladder and guide plasmid were stained with ethidium bromide and visualised using a UV transilluminator (324 nm). The body of the gel was then cut to individual sample lanes and the portion containing 2kb - 12 kb, as judged by the guide plasmid and ladder, was reset such that the first dimension ran left to right. This was set into a gel containing 1.2% agarose (4.8 g of Mega Sieve agarose in 400 ml 1x TBE buffer) and 1 μg/ml chloroquine. This second dimension gel was run, in 1x TBE also containing 1 μg/ml chloroquine, for 10 hours at 125 V at 4 °C.

Southern Blot Analysis

DNA was then transferred to the membrane using 20x SSC buffer and blotting paper and paper towels to draw the liquid through, left for a minimum of 10 hours. The membrane was transferred to a UV Stratalinker and auto-crosslinked (1200 J/cm2) DNA side up and uncovered and then washed in 5x SSC until hybridization.
The membrane was placed into a glass tube and incubated with 50 ml of blocking solution (0.1% SDS, 5% Dextrane sulphate, 5% Blocking liquid (GE), dissolved in 5x SSC) rolling at 65 °C for a minimum of 2 hours. The probe was denatured by boiling at 95 °C for 30 minutes and then left on ice to cool. The denatured probe was added in place of the blocking solution and left rolling at 65 °C overnight. The membranes were then washed twice in primary washing buffer (1x SSC, 0.1% SDS) for 15 minutes and then twice in secondary washing buffer (0.5x SSC, 0.1% SDS) for 10 minutes, all at 65 °C. The membrane was rinsed at room temperature in 50 ml of AB buffer (100 mM Tris-HCl, 150 mM NaCl, pH 7.5) and incubated in 250 ml of 1% milk powder in AB buffer at room temperature for 2 hours. Following blocking, the membrane was rinsed again in 50 ml AB buffer and then incubated in 250 ml of 0.5%

milk in AB buffer with 1:250,000 dilution of Anti-Fluorescein-AP Fab fragments (Roche) for 1 hour. Finally the membranes were washed three times in AB buffer with 0.2% Tween 20 (Sigma) for 10 minutes at room temperature and then incubated with CDP-Star® Detection reagent (GE) for 10 minutes at room temperature, followed by exposure to ECL Hyperfilm (GE Healthcare).

Chromatin Immunoprecipitation (ChIP) and CLK

For ChIP analysis 100 ml of culture at an OD600 of 1 were fixed with formaldehyde (final concentration of 1.42%) for 15 minutes at 25 °C, and quenched with glycine (final concentration 125 mM) for 5 minutes before the cells were harvested by centrifugation at 4,000 rpm for 2 minutes. The pellets were washed in PBS and transferred to a screw cap tube and frozen on dry ice. The pellets were stored at -80 °C. For CLK analysis, samples of 100 ml of culture at an OD600 of 1 were crosslinked with formaldehyde to a final concentration of 1.42% for times between 5 sec and 30 minutes at 25 °C before quenching with 250 mM glycine (twice that used for other ChIP) for 5 minutes and the cells collected as above. Pellets were resuspended in 100 µl of IP buffer (150 mM NaCl, 50 mM Tris-HCl (pH 7.5), 5 mM EDTA, NP-40 (0.5% v/v), Triton® X-100 (1% v/v)) containing phenylmethanesulfonyl fluoride (PMSF, final concentration 1 mM) and Complete protease inhibitor cocktail (without EDTA, from Roche), and 500 µl glass beads were added. Cells were broken by five 20 sec cycles, power setting 5.5 in a FastPrep® FP120 (BIO 101) machine with 1 min on ice after each second cycle. 300 µl IP buffer, containing PMSF and protease inhibitors, were then added, the tubes vortexed thoroughly and then pierced with a hot needle and placed into new eppendorfs and spun (2,000 rpm for 2 min) to collect the lysate. The cell lysate was spun down for 10

minutes at 13,000 rpm at 4 °C. This pellet was resuspended in 1 ml IP buffer containing PMSF and protease inhibitors, and this solution was sonicated for 1 hour (30 sec on, 30 sec off) at high power at 4 °C (Diagenode Bioruptor). Post-sonication, samples were spun down again for 10 minutes at 13,000 rpm, and the supernatant taken. 100 µl of sonicated chromatin were taken as 'input' and the remaining volume was divided between tubes for incubation with antibody. The 'input' DNA was precipitated with 0.3 M sodium acetate (NaOAc) and 2.5 volumes of cold ethanol and spun down at 15,000 rpm for 30 minutes, and the supernatant removed. The pellet was air dried, and then 250 µl of 10% (w/v) Chelex 100® suspension were added and the pellet fully resuspended at room temperature before boiling for 30 minutes. After boiling, the tubes were spun down at 6,000 rpm and the supernatant was cleaned using the PCR purification kit (Qiagen) according to the manufacturer's instructions. Finally, DNA was eluted in 250 µl of sterile distilled water. The main IP sample was incubated with the appropriate amount of antibody (anti-HA 12CA5 from Roche, anti-myc 9E10 from Sigma) for 30 minutes in an ultrasonic water bath on low power at 4 °C. After sonication, it was spun down at 13,000 rpm for 5 min, and the supernatant was added to a 100 µl slurry of 50:50 Protein A and Protein G beads (Roche), which had been equilibrated in IP buffer. The sample and beads were incubated for 2 hours at 4 °C and then the beads washed 4 times in IP buffer with inhibitors and twice more in IP buffer without inhibitors (spun 6,000 rpm for 1 minute in each wash, supernatant aspirated and 1.5 ml of washing buffer added and tubes inverted). After the final wash, 250 µl of 10% (w/v) Chelex 100® was added and samples boiled for 30 minutes. After a final spin at 6,000 rpm for 1 minute, the supernatant was transferred to a new tube and stored, along with the input DNA at 4 °C for short periods or -20 °C for up to several months.

Real time PCR (qPCR)

For each primer pair to be used, 7 µl of a primer mix (final concentration of 0.78 µM of each primer in nuclease free water), 3 µl of DNA from ChIP and 10 µl of Sensimix were added per well (Bioline). The plate was sealed and spun briefly to 1,500 rpm. Plates were then run in a CFX96 qPCR machine (Bio-Rad).

Quantification of IP signals

To eliminate background and non-specific enrichment due to high transcription regions (Teytelman et al., 2013) all analyses were done using tagged and untagged strains. First ChIP signals obtained for both tagged and isogenic untagged strains were each normalized to their respective input samples. Then signals for each primer pair from untagged strains were subtracted from those obtained for the tagged samples. The results obtained are presented as the percentages of the recovery over the input.

ChIP-seq

100 ml of culture at an OD600 of 0.5 were crosslinked for 30 min at room temperature with formaldehyde (final concentration 1%) then harvested by centrifugation and washed with TBS (50 mM Tris-Cl, pH 7.6, 150 mM NaCl) three times. Without freezing, the cell pellets were resuspended in 1.6 ml of Lysis buffer (50 mM Hepes-KOH pH 7.5, 140 mM NaCl, 1 mM EDTA, 1% Triton®-X100, 0.1% Sodium-deoxycholate , 1 mM PMSF and Complete protease inhibitor cocktail tablets (Roche)) and transferred to 2 ml screw cap tubes, glass beads added (Sigma G-8772) and cells broken with a multibeads shocker (Yasui-kikai) at 2700 rpm/min for 20

cycles of 1 min shaking + 1 min pause at 4 °C. The cell lysate was recovered and sonicated for 15 seconds for 5 times (Branson Sonifier 250D), and spun down to repellet the chromatin in between each round of sonication. The sheared chromatin was then spun at 15,000 rpm for 10 min at 4 °C and the supernatant taken to a new tube, where antibody-conjugated magnetic beads were added and incubated overnight at 4 °C. (20 µl of Dynabeads (Dynal) were washed twice with 0.5 ml cold PBS containing 5 mg/ml Bovine Serum Albumin (BSA), then resuspended in PBS/BSA and incubated with the appropriate amount of antibody for 4 hours, before being washed twice more with ice cold PBS/BSA. An aliquot of the chromatin was kept aside as an input fraction. Following overnight incubation of chromatin with the antibody conjugated beads, these were washed using a magnetic stand as follows: 2 x with 1 ml of ice cold Lysis buffer (w/o anti-proteolytics); 2 x with 1 ml of ice cold Lysis buffer plus 360 mM NaCl; 2 x with 1 ml of ice cold wash buffer (10 mM Tris-Cl pH 8, 250 mM LiCl, 0.5% NP-40, 0.5% Sodium-deoxycholate, 1 mM EDTA); and 1 x with 1 ml of ice cold TE (10 mM Tris-Cl pH 8, 1 mM EDTA, pH8). Finally, beads were spun down at 3,000 rpm for 1 min and the supernatant discarded. 100 µl of elution buffer were added (50 mM Tris-Cl pH 8, 10 mM EDTA, 1% SDS) and incubated at 65 °C for 10 min. The tubes were spun at 15,000 rpm for 1 min at room temperature and the supernatant taken to a new tube. The obtained ChIP DNA fraction as well as the input DNA was diluted with TE containing 1% SDS and incubated overnight at 65 °C in an oven to reverse the crosslinking. To clean up the DNA, Proteinase K was added to 0.5 mg/ml and glycogen to 0.2 mg/ml and incubated at 37 °C for 4 hours. Then NaCl was added to a final concentration of 200 mM before performing phenol/chloroform/iso-amylalcohol extraction. DNA was then precipitated by adding 2.5 volumes of cold ethanol, incubating at -20 °C overnight

before being spun down at 14,000 rpm for 30 min at 4 °C. The pellet was washed with 80% EtOH, dried and resuspended in 30 µl TE buffer containing 10 µg RNaseA, and incubated at 37 °C for 1 hour. After RNase treatment, the DNA was purifed by Qiagen PCR purification kit (Qiagen), eluted in 50 µl of distilled water. High-throughput sequencing was carried out using SOLiD 5500 (Applied Biosystems) system. DNA before and after ChIP (input and ChIP DNA, respectively) was processed and sequenced per the manufacturer's instructions. Briefly, DNA was sheared to an average size of ~150 bp by ultrasonication (Covaris), end-repaired, ligated to sequencing adapters, amplified, size-selected and sequenced to generate single-end 50-bp reads. Reads were aligned to the *S. cerevisiae* genome sequence using Bowtie (Langmead et al., 2009). Mapping results were processed and converted to genome-wide protein distribution profiles (ChIP-seq profiles) using parse2wig and DROMPA software as described (Sutani et al., 2015). The relative enrichment ratio (rER), which is a ratio of the number of ChIP sequence reads mapped at a specific 10-bp genome segment to the number of input sequence reads mapped at the same genome site, smoothened with a 500-bp size window and normalized to make the genome-wide average of rER values equal to 1, reflects accurately the degree of enrichment in the ChIP procedure, and were plotted along chromosomes. Full genome-wide ChIP-seq profiles are shown for all experiments done in Supplementary Figures 2-7.

Supplementary Data Legends

Data S1. Genome-wide association of condensin subunit Smc2 to yeast chromosomes in metaphase arrested cells (See Fig. 1A- *CDC20* metaphase arrest-plus nocodazole). Refers to main Figure 1.

Data S2. Genome-wide association of condensin subunit Smc2 to yeast chromosomes in metaphase arrested cells (See Fig. 1A- *CDC20* metaphase arrest-minus nocodazole). Refers to main Figure 1.

Data S3. Genome-wide association of condensin subunit Smc2 to yeast chromosomes in metaphase arrested cells (See Fig. 1A- *CDC20* metaphase arrest- nocodazole addback). Refers to main Figure 1.

Data S4. Genome-wide association of condensin subunit Smc2 to yeast chromosomes in G1 arrested cells (See Fig. 1B). Refers to main Figure 1.

Table S1: Yeast strains used in this study

Strain number	Genotype	Origin
CCG705	Mata; bar1Δ; smc2-8; leu2-3,112; ura3-52; his3- Δ 200; trp1- Δ 63;ade2-1; lys2-801	This study
CCG975	Mata; cdc5-1; leu2; ura3; his3; trp1	This study
CCG1835	Mata; bar1:hisG; ura3-1; trp1-1; leu2-3,112; his3-11; ade2-1; can1-100; GAL+; cdc15-2	This study
CCG4000	Mata; leu2-3,112; ura3-52; his3-Δ200; trp1-Δ63; ade2-1; lys2-801; bar1Δ; pep4:HIS3	This study

CCG9118	Mat a; ade2-1; his3-11; leu2-3; trp1-1; ura3-1; can1-100; UBR1::GAL-10-Ubiquitin-M-LacI fragment-myc-UBR1 (His3); leu2-3::pCM244 (CMVp-tetR'-SSN6 LEU2) x3; top2td TOP2 5' upstream -100 to -1 replaced with kanMX-tTA (tetR-VP16)-tetO$_2$ - Ub - DHFRts - myc - linker)	Baxter *et al*, 2011
CCG9120	Mat a; ade2-1; his3-11; leu2-3; trp1-1; ura3-1; can1-100; UBR1::GAL-10-Ubiquitin-M-LacI fragment-myc-UBR1 (His3); leu2-3::pCM244 (CMVp-tetR'-SSN6 LEU2) x3; top2td TOP2 5' upstream -100 to -1 replaced with kanMX-tTA (tetR-VP16)-tetO$_2$ - Ub - DHFRts - myc - linker); pRS316 (ura3)	Baxter *et al*, 2011
CCG9121	Mat a; ade2-1; his3-11; leu2-3; trp1-1; ura3-1; can1-100; UBR1::GAL-10-Ubiquitin-M-LacI fragment-myc-UBR1 (His3); leu2-3::pCM244 (CMVp-tetR'-SSN6 LEU2) x3; top2td TOP2 5' upstream -100 to -1 replaced with kanMX-tTA (tetR-VP16)-tetO$_2$ - Ub - DHFRts - myc - linker); cdc15-2; pRS316 (ura3)	Baxter *et al*, 2011
CCG9126	Mat a; ade2-1; his3-11; leu2-3; trp1-1; ura3-1; can1-100; UBR1::GAL-10-Ubiquitin-M-LacI fragment-myc-UBR1 (His3); leu2-3::pCM244 (CMVp-tetR'-SSN6 LEU2) x3; top2td TOP2 5' upstream -100 to -1 replaced with kanMX-tTA (tetR-VP16)-tetO$_2$ - Ub - DHFRts - myc - linker); cdc20-td CDC20 5' upstream -100 to -1 replaced with KanMX-tTA (tetR-VP16)-tetO$_2$ - Ub - DHFRts - myc - linker); pRS316 (URA3)	Baxter *et al*, 2011
CCG9335	Mata; leu2-3,112; ura3-52; his3-Δ200; trp1-Δ63; ade2-1; lys2-801; bar1Δ; pep4:HIS3; smc2-6HA (KanMX)	This study
CCG9513	Mata; bar1:hisG; ura3-1; trp1-1; leu2-3,112; his3-11; ade2-1; can1-100; GAL+; cdc15-2; smc2-6HA (KanMX)	This study
CCG9423	Mat a; ade2-1; his3-11; leu2-3; trp1-1; ura3-1; can1-100; UBR1::GAL-10-Ubiquitin-M-LacI fragment-myc-UBR1 (His3); leu2-3::pCM244 (CMVp-tetR'-SSN6 LEU2) x3; top2td TOP2 5' upstream -100 to -1 replaced with kanMX-tTA (tetR-VP16)-tetO$_2$ - Ub - DHFRts - myc - linker); cdc20-td CDC20 5' upstream -100 to -1 replaced with KanMX-tTA (tetR-VP16)-tetO$_2$ - Ub - DHFRts - myc - linker); pRS316 (URA3); cdc5-1 (ade2)	This study
CCG9767	Mat a; ade2-1; his3-11; leu2-3; trp1-1; ura3-1; can1-100; UBR1::GAL-10-Ubiquitin-M-LacI fragment-myc-UBR1 (His3); leu2-3::pCM244 (CMVp-tetR'-SSN6 LEU2) x3; top2td TOP2 5' upstream -100 to -1 replaced with kanMX-tTA (tetR-VP16)-tetO$_2$ - Ub - DHFRts - myc - linker); cdc20-td CDC20 5' upstream -100 to -1 replaced with KanMX-tTA (tetR-VP16)-tetO$_2$ - Ub - DHFRts - myc - linker); ipl1-321 (ura); pRS414 (trp)	This study
CCG10013	Mat a; ade2-1; his3-11; leu2-3; trp1-1; ura3-1; can1-100; UBR1::GAL-10-Ubiquitin-M-LacI fragment-myc-UBR1 (His3); leu2-3::pCM244 (CMVp-tetR'-SSN6 LEU2) x3; top2td TOP2 5' upstream -100 to -1 replaced with kanMX-tTA (tetR-VP16)-tetO$_2$ - Ub - DHFRts - myc - linker); cdc20-td CDC20 5' upstream -100 to -1 replaced with KanMX-tTA (tetR-VP16)-tetO$_2$ - Ub - DHFRts - myc - linker); dyn1Δ::NAT; kip1Δ::Hyg; cyn8-3 (trp); pRS316 (URA3)	This study
CCG10429	Mata; leu2-3,112; ura3-52; his3-Δ200; trp1-Δ63; ade2-1; lys2-801; bar1Δ; pep4:HIS3; smc2-9myc (hyg)	This study
CCG10488	Mata; leu2-3,112; ura3-52; his3-Δ200; trp1-Δ63; ade2-1; lys2-801; bar1Δ; pep4:HIS3; pMET-cdc20 (trp)	This study
CCG10490	Mata; leu2-3,112; ura3-52; his3-Δ200; trp1-Δ63; ade2-1; lys2-801; bar1; pep4:HIS3; smc2-9myc (hyg); pMET-cdc20(trp)	This study
CCG11726	Mata; leu2-3,112; ura3-52; his3-Δ200; trp1-Δ63; ade2-1; lys2-801; bar1Δ; pep4:HIS3; smc2-6HA (KanMX); pMET-cdc20 (trp)	This study
CCG11772	Mata cdc5-1 leu2 ura3 his3 trp ; smc2-6HA hyg	This study

CCG11904	Mata; bar1:hisG; ura3-1; trp1-1; leu2-3,112; his3-11; ade2-1; can1-100; GAL+; cdc15-2; top2-6HA (hyg)	This study
CCG11978	Mata cdc5-1 leu2 ura3 his3 trp ; Smc2-6HA	This study
CCG12260	Mata; leu2-3,112; ura3-52; his3-Δ200; trp1-Δ63; ade2-1; lys2-801; bar1Δ; pep4:HIS3; top2-4 (ade2); smc2-6HA (hyg)	This study
CCG12263	Mata; leu2-3,112; ura3-52; his3-Δ200; trp1-Δ63; ade2-1; lys2-801; bar1Δ; pep4:HIS3; brn1-9myc (trp); smc2-6HA (hyg)	This study
CCG9704	Mat a; ade2-1; his3-11; leu2-3; trp1-1; ura3-1; can1-100; UBR1::GAL-10-Ubiquitin-M-LacI fragment-myc-UBR1 (His3); leu2-3::pCM244 (CMVp-tetR'-SSN6 LEU2) x3; top2td TOP2 5' upstream -100 to -1 replaced with kanMX-tTA (tetR-VP16)-tetO2 - Ub - DHFRts - myc - linker); cdc20-td CDC20 5' upstream -100 to -1 replaced with KanMX-tTA (tetR-VP16)-tetO2 - Ub - DHFRts - myc - linker); brn1-60; pRS316 (URA3)	This study

Table S2: Primers used in this study

Primer number	Target	Forward primer (5' – 3')	Reverse primer (5' – 3')
3689 3670	CEN4 (0)	TGCTTGCAAAAGGTCACATGCTTAT	CATTTTGGCCGCTCCTAGGTAGTG
3494 3495	HMR	AAATCAATCTCAATACTAATAATCTTTA	GAGTAATGCCACATTTCTTTGCAAC
3520 3521	CEN4 -450	CAGCGCGTTTCACTTTTAAATCAAA	TTGCATGATCAAAAGGCTCAATGTT
3623 3624	CEN4 +125	CACTACCTAGGAGCGGCCAAAATG	ACGATAAAACCGGAAGGAAGAATAA
3625 3626	CEN4 +450	AAAATCCAATTGTTGATGAACCTCA	AGAAGAGCGCTTGGTGCTTGCAT
3627 3628	CEN4 +700	AATAACCATAAGAACGGAGGCCTTCCC	CCGCAACTACATTCTGGGCATTATG
3629 3630	CEN4 right	CAAAACCTTCAGTAGCTGCCCCTTTAA	CCGCAACTACATTCTGGGCATTATG
3713 3714	CEN12 (0)	TAAGGAGAAAACTTGTAGTACGAGGT	GTTGAATATTTGAAGTACACACCCGC
3777 3778	Chrm IV +100kb	AAATGTTAATGGGAGTGGCGC	ATGAAACTGTTGTTCGGACCG
3779 3780	ChrmIV +50kb	CTGGAAGTAGTAGATGAAGCC	TCTGATGATGAAGAACACGGC
3781 3882	ChrmIV +15kb	ATCGTTGGCCACCAATTGTTG	AGGAAGATGGTGAGAGAGTAC

3963 3964	20Kb (Chr XII)	AGTTGCTAACGAACAGGATGG	TTGGTACAAAAGCCTTGTCCC
3967 3968	225Kb (Chr XII)	GAGAAGAATGATTCTCGCAGC	TACTGATGGAATCGTTGTCCG
3971 3972	450Kb (Chr XII)	CTTGTTCTGCTTCGCCAATTG	GTTCGGAGTTCCATTCATCTC
3973 3974	900Kb (Chr XII)	CTGGATTGGCGCATTTCTGCGAG	ATTGGTCAAAGACTTGTCTAATTGGTA
3979 3980	500Kb (Chr XII)	GCTCACTAGAAAACTTGACCG	TTCACAGGAAGCCCAGAAAAC

3975 3976	rDNA	CGCAAAAGAAACACACTCTGG	TGTAAATGGCCTCGTCAAACG